www.sciencemag.org/content/362/6415/686/suppl/DC1

Supplementary Materials for

Heterogeneity in efflux pump expression predisposes antibiotic-resistant cells to mutation

Imane El Meouche and Mary J. Dunlop*

*Corresponding author. Email: mjdunlop@bu.edu

Published 9 November 2018, *Science* **362**, 686 (2018)
DOI: 10.1126/science.aar7981

This PDF file includes:

Other Supplementary Material for this manuscript includes the following:
(available at www.sciencemag.org/content/362/6415/686/suppl/DC1)

Materials and Methods

Strains and plasmids

E. coli strains used in this study are derived from K-12 MG1655 (*38*) and K-12 BW25113 (*39, 40*). The strains JW0451-2 (Δ*acrB*) and JW2703-2 (Δ*mutS*) were obtained from the Keio collection (*40*). The kanamycin resistance marker gene was removed from the Keio collection strains using the pCP20 plasmid (*39*). The *S.* Typhimurium LT2 strain is derived from Ref. (*41*). The original strain contained a temperature sensitive plasmid pKD46. This plasmid was removed by growing bacteria for two overnight cycles at 42°C and loss of the plasmid was verified by plating on carbenicillin.

All plasmids described below were constructed using the Gibson assembly method (*42*).

P_{lac}-*acrAB*

The plasmid overexpressing *acrAB* from an inducible lacUV5 promoter was obtained from Ref. (*43*).

P_{lac}-*acrAB* F610A

Modification of the 610th amino acid in *acrB* (*19*) was realized using site directed mutagenesis using the primers GCAGCCGTTAACGGCTTCG and CACCGA CTCAACGTTGTTCTT. The plasmid overexpressing the catalytically compromised *acrAB* F610A from an inducible lacUV5 promoter was then introduced in the Δ*acrB* strain.

P_{lac}-*cfp*

The *cfp* gene tagged with an *ssrA* tag described in Ref. (*5*) was cloned into the medium-copy (SC101) origin, carbenicillin and kanamycin resistant vectors pBbA5a and pBbA5k (*44*) using the primers ATGACTAGCAAAAGAAGC and CTATTACGCTGCAAGGG.

P_{acrAB}-*rfp* + P_{mutS}-*yfp*

The *mutS* promoter region was amplified from the *E. coli* chromosome using the primers GCGTACTTGCTTCATAAGCATCA and ACATGATACCGGAGTTAATCA. The *acrAB* promoter region was amplified using GCCAGTAGATTGCACCGCG and TCGTGCTATGGTACATACATTCACA (*32*). The promoter sequences were cloned upstream of *yfp* and *rfp* from Ref. (*45*) and inserted into a vector with SC101 origin and kanamycin resistance from Ref. (*44*).

P_{acrAB}-*acrAB*-*rfp* + P_{mutS}-*mutS*-*yfp*

The *acrAB* operon with linker from Ref. (*7*) was inserted in the double color plasmid P_{acrAB}-*rfp* + P_{mutS}-*yfp* described above using the primers TCCCTGTCCTTTGTTACCGG and ATGAACAAAAACAGAGGGT. The P_{mutS} promoter and *mutS* gene were then inserted with the same linker as used in *acrAB*-*rfp* into the plasmid P_{acrAB}-*acrAB*-*rfp* + P_{mutS}-*yfp* using the primers GCGTACTTGCTTCATAAGCATCACGCA and CACCAGGCTCTTCAAGCGATAAATCCA to obtain the final translational fusion construct. The C-terminal fusion of AcrAB-RFP is based on Ref. (*7*) and the C-terminal fusion of MutS-YFP is based on Ref. (*21*).

P_{const}-*rfp* + P_{mutS}-*yfp*
The P_{acrAB} promoter was replaced with a constitutive promoter from Ref. (*46*) using the primers GTGTCCCTCTCGATGGCTG and TTATCAAAAAGAGTATTGACA. Specifically, the promoter used here is a variant of the σ70 consensus sequence: TTATCAAAAAGAGTATTGACATAAAGTCTAACCTATAGGAGTATTACAGCC**A**TC where the +1 transcriptional start site is shown in bold and the -10 and -35 regions are underlined.

P_{acrAB}-*rfp* + P_{const}-*yfp*
The P_{mutS} promoter was replaced with the constitutive promoter described above using the primers TTATCAAAAAGAGTATTGACA and GTGTCCCTCTCGATGGCTG.

P_{marA}-*cfp*
The plasmid containing the promoter of the *marRAB* operon with the *ssrA* tagged CFP gene was obtained from Ref. (*5*).

P_{const}-*cfp*
The constitutive promoter was obtained from Ref. (*47*) and was cloned on the low-copy (SC101) origin, kanamycin resistant vector pBbS5k harboring *ssrA* tagged CFP from Ref. (*5*).

P_{lac}-*marA*
The *marA* sequence was amplified from *E. coli* MG1655 genomic DNA (*5*). This sequence was then cloned into the medium copy (p15A) origin, carbenicillin resistant vector pBbA5a (*44*).

Spontaneous mutation frequency
Overnight cultures were inoculated from single colonies in Luria Bertani (LB) medium with 30 μg/ml kanamycin or 100 μg/ml carbenicillin as required for reporter plasmid maintenance. The control strains without *acrAB* overexpression contained an equivalent plasmid expressing CFP (P_{lac}-*cfp*) in place of *acrAB*. Overnight cultures were diluted 1:1,000,000 and incubated at 37°C with shaking until mid-exponential phase (OD_{600nm} = 1.3). This extreme dilution minimizes the presence of pre-existing stationary phase mutants. The total number of colony forming units per ml (CFU/ml) was determined by plating on LB agar. To count mutants, cells were centrifuged and plated on LB agar with 100 μg/ml rifampicin, 0.1 μg/ml ciprofloxacin, 6 μg/ml tetracycline, or 5 μg/ml chloramphenicol. LB plates were incubated 24 hours at 37°C and selective plates were incubated 48-72 hours at 37°C (*48*). The mutation frequency was then determined as the CFU/ml on LB + selective antibiotic agar plates divided by the CFU/ml on LB agar plates. We used the Mann-Whitney rank sum test to determine statistical significance.

For *S.* Typhimurium LT2, overnight cultures were diluted 1:10,000 and incubated at 37°C with shaking until mid-exponential phase. A lower dilution was used in these experiments because *acrAB* expression increased the time for cells to reach mid-exponential phase in *Salmonella* relative to *E. coli*. Two hours before plating cells, we added 15 μM IPTG to the cultures to induce *acrAB* expression.

Calculating mutation rates

Mutation rates were calculated based on the Ma–Sandri–Sarkar maximum-likelihood method (*49*) using the FALCOR web tool (*50*).

Determination of the minimum inhibitory concentration

Overnight cultures were diluted and incubated at 37°C for 4 hours with shaking. Cells were then diluted 1:100 and incubated with increasing concentrations of ciprofloxacin, tetracycline, or chloramphenicol at 37°C for 20 hours with shaking. The minimum inhibitory concentration was determined as the concentration of antibiotic where no visible growth was observed. For the disc diffusion method, overnight cultures were diluted and incubated until exponential phase. They were then plated homogeneously on LB plates using sterile swabs and ciprofloxacin disc (5 μg/ml Oxiod^{TM}) were placed on top. Plates were then incubated overnight to observe growth inhibition, as indicated by the size of the zone of clearance surrounding the disc.

Single-cell fluorescence and time-lapse microscopy

Cultures were inoculated from single colonies in LB medium with 30 μg/ml kanamycin or 100 μg/ml carbenicillin, where required for plasmid maintenance. Overnight cultures were diluted 1:100 and incubated at 37°C with shaking until mid-exponential phase (OD_{600nm} = 1.3). Cells were then placed on 1.5% MGC low melting temperature agarose pads. MGC is M9 minimal medium containing 0.2% glycerol, 0.01% casamino acids, 0.15 μg/ml biotin, and 1.5 μM thiamine. Cells were then imaged at 100× using a Nikon Instruments Ti-E microscope. Phase contrast, YFP, and RFP images were taken. For the movies, the temperature of the microscope chamber was held at 32°C for the duration of the experiment and images were collected every 5 minutes. Image analysis and growth rate measurements were done using the SuperSegger Matlab-based cell segmentation program (*51*). Growth of single cells is exponential (*52*), thus, we calculated growth rate as the natural log of the ratio of the length of the cell at the end of the lineage to its length at the start of the lineage, divided by the length of the lineage in minutes.

Fluorescent activated cell sorting

A BD FACSAria II instrument and a BD FACSAria III instrument equipped with a 405 nm laser and a 70 μm nozzle (70 psi) were used. After growing *E. coli* strains containing P_{marA}-*cfp* or P_{const}-*cfp* until mid-exponential phase (OD_{600nm} = 1.3), cells were subjected to sorting. A neutral density-1 filter was used to collect the FSC signal, and the CFP fluorescence signal was collected using a 525/50 bandpass filter. Cells were sorted based on intensity of the CFP signal. An *E. coli* strain without a plasmid was used as a control to set up a negative/positive gate. A total of 500,000 cells (corresponding to the lowest and highest ~10% of the population) were collected to generate 'low' and 'high' sub-populations and were then grown until mid-exponential phase at 37°C in LB with shaking. Cells were then diluted and plated on LB and LB + 100 μg/ml rifampicin agar plates. We used the Mann-Whitney rank sum test to determine statistical significance. Data were acquired using BD FACSDiva software v8.0.1 and analyzed with FlowJo software version 10 (FlowJo, LLC, Ashland, OR).

Supplementary Text

MarA overexpression leads to elevated mutation frequencies via AcrAB

Using fluorescence-activated cell sorting, we sorted wild type *E. coli* into subpopulations with low and high MarA expression using a cyan fluorescent protein reporter, P_{marA}-*cfp* (*5*) (Fig. S8A). Within a population of wild type cells we observed a correlation between *marA* expression and the spontaneous mutation frequency (Fig. S8B). We found that cells from the top ~10% of *marA* expression levels had higher mutation frequencies than those from the bottom ~10% (Fig. S8B). As a negative control, we performed the same experiment with cells containing a constitutive promoter, P_{const}-*cfp*, and found similar mutation frequencies in the top and bottom ~10% of sorted cells (Fig. S8C). This result shows that pre-existing variability in *marA* predisposes bacteria to different mutation rates. To confirm this effect at the population level, we introduced a plasmid containing *marA* in *E. coli*. We found higher mutation frequencies in the strain overexpressing *marA* than in wild type cells (Fig. S8D).

MarA controls over 60 downstream genes in addition to *acrAB* (*29*), therefore we asked whether MarA itself or other genes besides *acrAB* play a role in increasing the mutation frequency. When we complemented the Δ*acrB* mutant with a plasmid overexpressing *marA* we did not find a significant increase in mutations (Fig. S8E). Thus, the increase in mutation frequency when MarA is overexpressed depends predominantly on AcrAB.

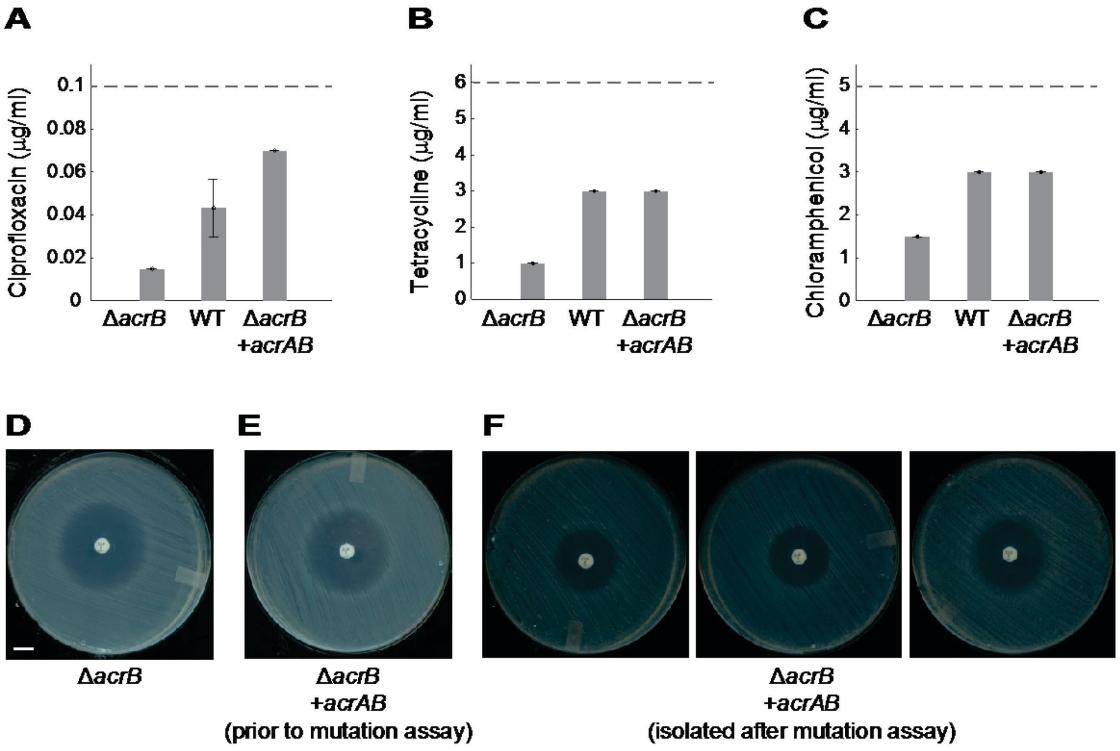

Fig. S1. Minimum inhibitory concentration measurements. (A-C) Minimum inhibitory concentration of (A) ciprofloxacin, (B) tetracycline, and (C) chloramphenicol for Δ*acrB*, wild type, and Δ*acrB* complemented with a plasmid overexpressing *acrAB*. Error bars ± SEM, n = 3 biological replicates. Dashed lines show antibiotic concentrations used for mutation assays in Fig. 1D, which are above the minimum inhibitory concentrations of all strains. **(D-F)** Ciprofloxacin resistance test using antibiotic discs where size of zone of clearance indicates level of antibiotic resistance (smaller = more resistant). Scale bar, 1cm. (D) Δ*acrB* and (E) Δ*acrB* complemented with a plasmid overexpressing *acrAB* for strains from before the ciprofloxacin mutation assay. (F) Representative examples of mutant strains isolated from the Δ*acrB* + *acrAB* mutation assay. These strains exhibit higher antibiotic resistance than the parent strain. The Δ*acrB* and wild type strains contain an equivalent plasmid expressing *cfp* in place of *acrAB*.

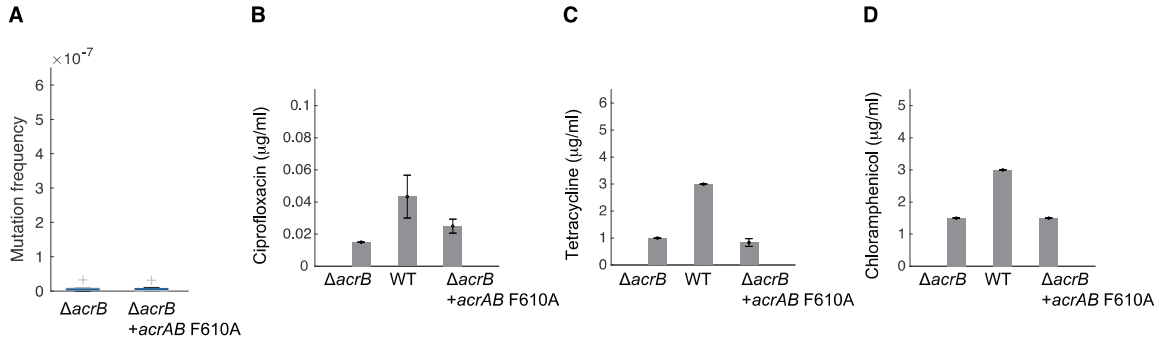

Fig. S2. Mutation frequency and minimum inhibitory concentration data for catalytically compromised AcrB. (A) Rifampicin mutation frequency in Δ*acrB E. coli* with and without *acrAB* overexpression. n ≥ 7 biological replicates. Blue bars show the median values, grey boxes indicate the interquartile range, and whiskers show the maximum and minimum values. Box plot raw data, Fig. S9B. Strain without *acrAB* overexpression contains an equivalent plasmid expressing *cfp* in place of *acrAB* F610A. Differences between two strains are not statistically significant, Mann-Whitney rank sum test. **(B-D)** Minimum inhibitory concentration of (B) ciprofloxacin, (C) tetracycline, and (D) chloramphenicol verifying loss of antibiotic resistance in the catalytically compromised AcrB F610A mutant. The Δ*acrB* and wild type strains contain an equivalent plasmid expressing *cfp* in place of *acrAB*. Error bars ± SEM, n = 3 biological replicates.

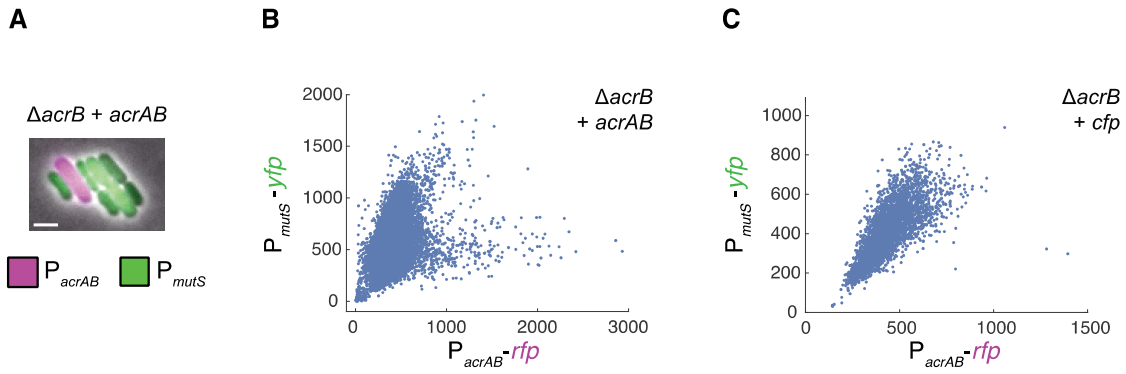

Fig. S3. Inverse relationship between P_{acrAB} and P_{mutS} expression in Δ*acrB* complemented with a plasmid overexpressing *acrAB*. **(A)** Fluorescence microscopy image of Δ*acrB* complemented with a plasmid overexpressing *acrAB* containing the reporter double color P_{acrAB}-*rfp* + P_{mutS}-*yfp*. Scale bar, 2μm. **(B)** RFP fluorescence levels reflecting *acrAB* promoter activity versus YFP fluorescence levels reflecting *mutS* promoter activity. Each dot corresponds to one cell. **(C)** Negative control with P_{acrAB}-*rfp* + P_{mutS}-*yfp* reporter in Δ*acrB* complemented with a plasmid overexpressing *cfp* instead of *acrAB*.

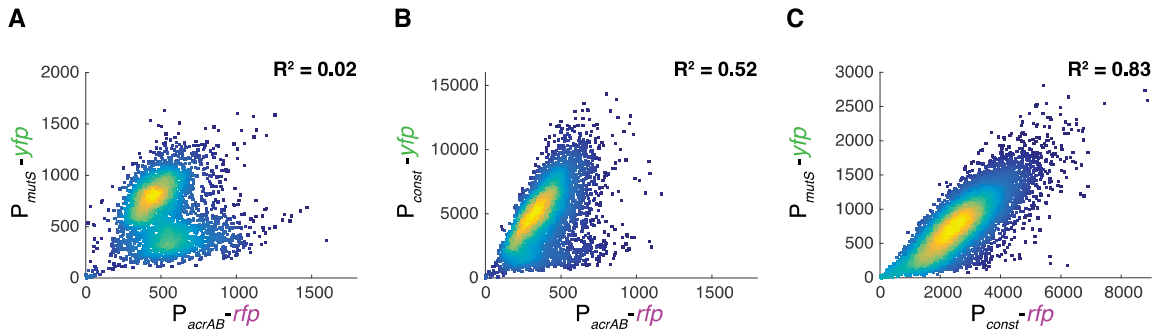

Fig. S4. Constitutive reporter controls. (A) RFP fluorescence levels reflecting *acrAB* promoter activity versus YFP fluorescence levels reflecting *mutS* promoter activity. **(B)** Equivalent experiments to (A), but with P_{mutS} replaced by a constitutive promoter P_{const}. **(C)** Equivalent to (A), but with P_{acrAB} replaced by P_{const}. R^2 values for a linear regression are noted in the top corner of each plot. Note that the reciprocal relationship observed in the P_{acrAB}-*rfp* vs. P_{mutS}-*yfp* data is not present in the controls. Fluorescence data are background subtracted. Each dot corresponds to one cell.

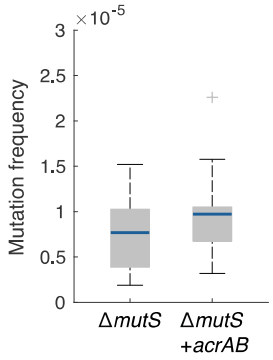

Fig. S5. Spontaneous rifampicin mutations in the Δ*mutS* strain. Rifampicin mutation frequency in Δ*mutS* strain with and without a plasmid overexpressing *acrAB*. Strain without *acrAB* contains the same plasmid expressing *cfp* in place of *acrAB*. Blue bars show the median values, grey boxes indicate the interquartile range, and whiskers show the maximum and minimum values for n = 11 biological replicates. Differences between two strains are not statistically significant, Mann-Whitney rank sum test. Mutation rates per generation are listed in Table S1. Raw data for the box plots are shown in Fig. S9C.

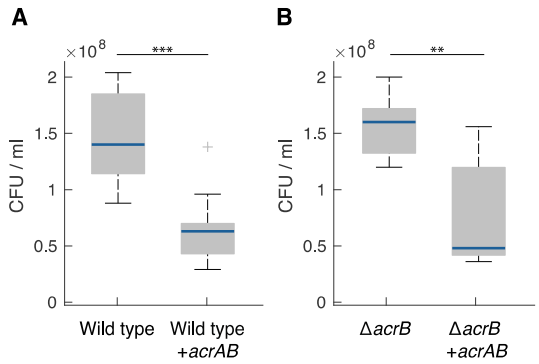

Fig. S6. Overexpression of *acrAB* decreases total cell counts. Colony forming units per milliliter (CFU/ml) for the following strains: **(A)** wild type with a plasmid overexpressing *cfp* and wild type with a plasmid overexpressing *acrAB* and **(B)** Δ*acrB* with a plasmid overexpressing *cfp* and Δ*acrB* with a plasmid overexpressing *acrAB*. Blue bars show the median values, grey boxes indicate the interquartile range, and whiskers show the maximum and minimum values. The differences in CFU/ml are statistically different in strains overexpressing *acrAB* ($P < 0.001$ for wild type and $P < 0.01$ for Δ*acrB* by Mann-Whitney rank sum test). Raw data for the box plots are shown in Fig. S9D. Data come from $n \geq 8$ biological replicates.

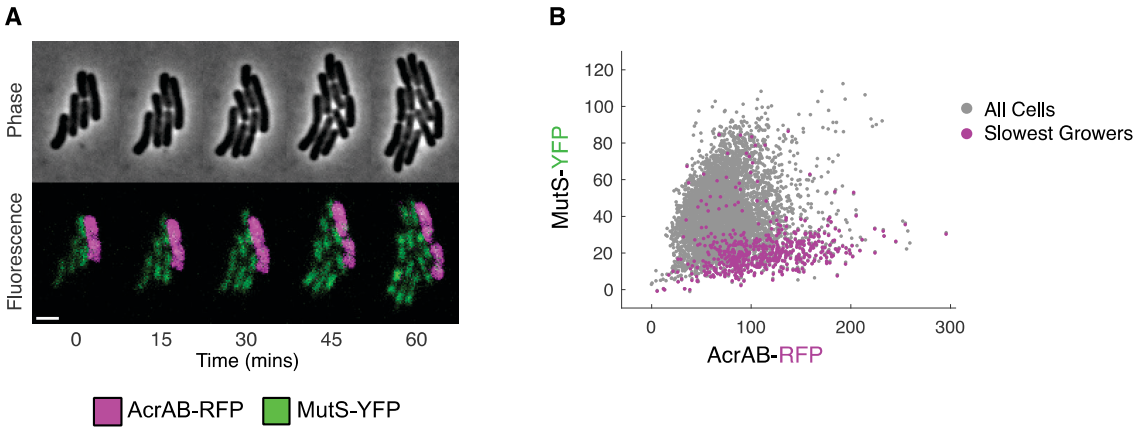

Fig. S7. AcrAB-RFP and MutS-YFP translational fusions. (A) Time-lapse microscopy images of wild type cells expressing the translational fusion P_{acrAB}-*acrAB-rfp* + P_{mutS}-*mutS-yfp*. Cells were imaged over 75 minutes in YFP and RFP channels (Movie S2). Scale bar, 2µm. **(B)** P_{acrAB}-*acrAB-rfp* versus P_{mutS}-*mutS-yfp*. Each dot corresponds to one cell. The purple dots correspond to cells whose growth rate falls in the bottom 10% of those measured. Fluorescence data are background subtracted.

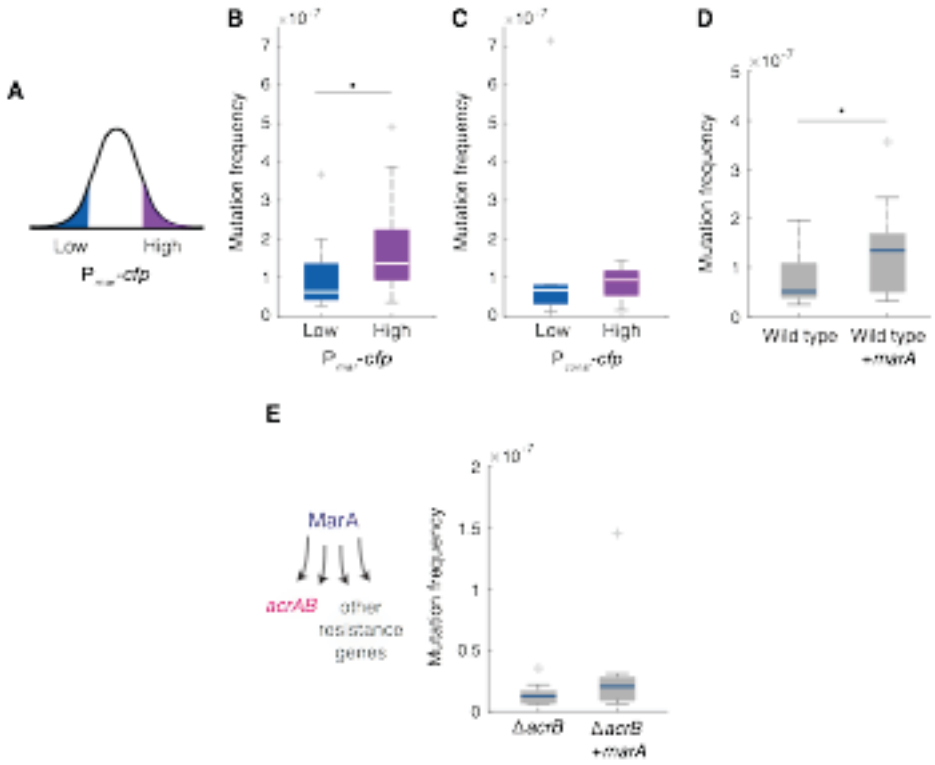

Fig. S8. Pre-existing cell-to-cell variation in *marA* expression correlates with spontaneous mutations. (A) Schematic illustrating the two fractions of cells sorted based on low and high P_{marA}-*cfp* expression. **(B)** Rifampicin mutation frequency in sorted cells containing low and high levels of CFP expressed from the *marA* promoter. **(C)** Rifampicin mutation frequency in sorted cells containing low and high levels of CFP expressed from a constitutive promoter. For (B-C) white bars show the median values, shaded boxes indicate the interquartile range, and whiskers show the maximum and minimum values. Data come from n ≥ 6 biological replicates. **(D)** Rifampicin mutation frequency in *E. coli* wild type cells with and without a plasmid overexpressing *marA*. Cells without *marA* overexpression contain an identical plasmid with *cfp* in place of *marA*. Data come from n ≥ 8 biological replicates. **(E)** Rifampicin mutation frequency in *E. coli* Δ*acrB* with and without a plasmid overexpressing *marA* from n ≥ 8 biological replicates. Mutation frequencies are not significantly different, Mann-Whitney rank sum test. For (D-E) blue bars show the median values, grey boxes indicate the interquartile range, and whiskers show the maximum and minimum values. Mutation rates per generation are listed in Table S1. Raw data for the box plots are shown in Fig. S9E. Mutation rates per generation are listed in Table S1. * = $P < 0.05$, one-tailed Mann-Whitney rank sum test.

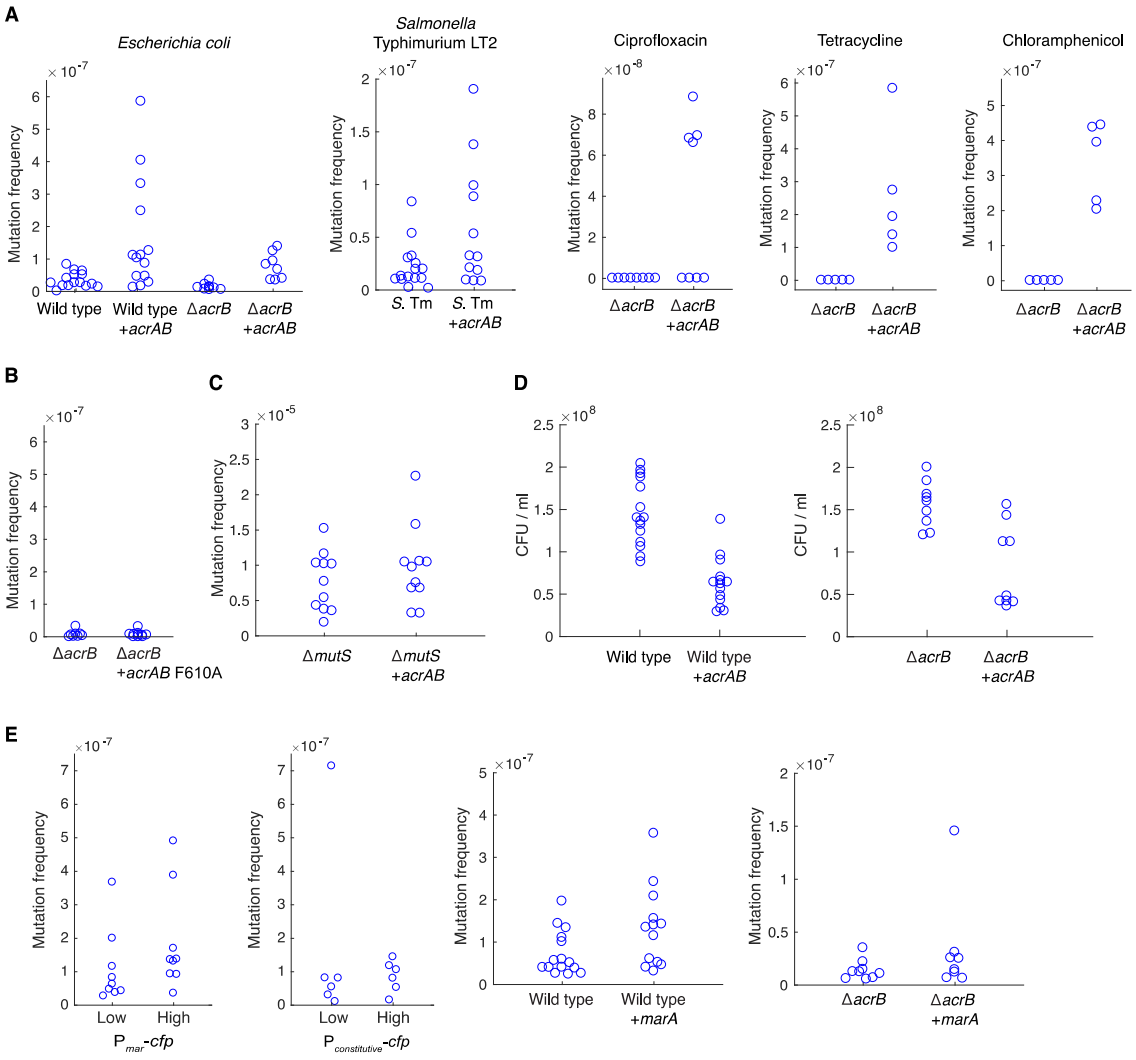

Fig. S9. Raw data from box plots. Raw data from the box plots in **(A)** Fig. 1, **(B)** Fig. S2, **(C)** Fig. S5, **(D)** Fig. S6, and **(E)** Fig. S8.

Table S1.
Mutation rates per generation for rifampicin.

Table S2.
Mutations in the *rpoB* gene from colonies isolated on rifampicin.

Movie S1

Time-lapse movie showing cell-to-cell variability in *acrAB* expression, *mutS* expression, and growth in wild type cells. Images were taken every 5 mins. Scale bar, 2μm. RFP levels showing *acrAB* promoter activity are indicated in magenta, YFP levels showing *mutS* promoter activity are indicated in green.

Movie S2

Time-lapse movie showing cell-to-cell variability in AcrAB-RFP, MutS-YFP, and growth. Images were taken every 5 mins. Scale bar, 2μm. RFP levels are indicated in magenta, YFP levels are indicated in green.

Movie S3

Time-lapse movie showing cell-to-cell variability in *acrAB* expression, *mutS* expression, and growth in the Δ*acrB* strain. Images were taken every 5 mins. Scale bar, 2μm. RFP levels showing *acrAB* promoter activity are indicated in magenta, YFP levels showing *mutS* promoter activity are indicated in green.

References and Notes

1. M. N. Alekshun, S. B. Levy, Molecular mechanisms of antibacterial multidrug resistance. *Cell* **128**, 1037–1050 (2007). doi:10.1016/j.cell.2007.03.004 Medline

2. B. R. Levin, D. E. Rozen, Non-inherited antibiotic resistance. *Nat. Rev. Microbiol.* **4**, 556–562 (2006). doi:10.1038/nrmicro1445 Medline

3. L. R. Mulcahy, J. L. Burns, S. Lory, K. Lewis, Emergence of *Pseudomonas aeruginosa* strains producing high levels of persister cells in patients with cystic fibrosis. *J. Bacteriol.* **192**, 6191–6199 (2010). doi:10.1128/JB.01651-09 Medline

4. N. Q. Balaban, J. Merrin, R. Chait, L. Kowalik, S. Leibler, Bacterial persistence as a phenotypic switch. *Science* **305**, 1622–1625 (2004). doi:10.1126/science.1099390 Medline

5. I. El Meouche, Y. Siu, M. J. Dunlop, Stochastic expression of a multiple antibiotic resistance activator confers transient resistance in single cells. *Sci. Rep.* **6**, 19538 (2016). doi:10.1038/srep19538 Medline

6. Y. Pu, Z. Zhao, Y. Li, J. Zou, Q. Ma, Y. Zhao, Y. Ke, Y. Zhu, H. Chen, M. A. B. Baker, H. Ge, Y. Sun, X. S. Xie, F. Bai, Enhanced efflux activity facilitates drug tolerance in dormant bacterial cells. *Mol. Cell* **62**, 284–294 (2016). doi:10.1016/j.molcel.2016.03.035 Medline

7. T. Bergmiller, A. M. C. Andersson, K. Tomasek, E. Balleza, D. J. Kiviet, R. Hauschild, G. Tkačik, C. C. Guet, Biased partitioning of the multidrug efflux pump AcrAB-TolC underlies long-lived phenotypic heterogeneity. *Science* **356**, 311–315 (2017). doi:10.1126/science.aaf4762 Medline

8. I. Levin-Reisman, I. Ronin, O. Gefen, I. Braniss, N. Shoresh, N. Q. Balaban, Antibiotic tolerance facilitates the evolution of resistance. *Science* **355**, 826–830 (2017). doi:10.1126/science.aaj2191 Medline

9. A. A. Al Mamun, M.-J. Lombardo, C. Shee, A. M. Lisewski, C. Gonzalez, D. Lin, R. B. Nehring, C. Saint-Ruf, J. L. Gibson, R. L. Frisch, O. Lichtarge, P. J. Hastings, S. M. Rosenberg, Identity and function of a large gene network underlying mutagenic repair of DNA breaks. *Science* **338**, 1344–1348 (2012). doi:10.1126/science.1226683 Medline

10. X. Z. Li, P. Plésiat, H. Nikaido, The challenge of efflux-mediated antibiotic resistance in Gram-negative bacteria. *Clin. Microbiol. Rev.* **28**, 337–418 (2015). doi:10.1128/CMR.00117-14 Medline

11. E. C. Hobbs, X. Yin, B. J. Paul, J. L. Astarita, G. Storz, Conserved small protein associates with the multidrug efflux pump AcrB and differentially affects antibiotic resistance. *Proc. Natl. Acad. Sci. U.S.A.* **109**, 16696–16701 (2012). doi:10.1073/pnas.1210093109 Medline

12. E. B. Tikhonova, H. I. Zgurskaya, AcrA, AcrB, and TolC of *Escherichia coli* form a stable intermembrane multidrug efflux complex. *J. Biol. Chem.* **279**, 32116–32124 (2004). doi:10.1074/jbc.M402230200 Medline

13. R. Krašovec, R. V. Belavkin, J. A. D. Aston, A. Channon, E. Aston, B. M. Rash, M. Kadirvel, S. Forbes, C. G. Knight, Mutation rate plasticity in rifampicin resistance depends on *Escherichia coli* cell-cell interactions. *Nat. Commun.* **5**, 3742 (2014). doi:10.1038/ncomms4742 Medline

14. A. M. Langevin, M. J. Dunlop, Stress introduction rate alters the benefit of AcrAB-TolC efflux pumps. *J. Bacteriol.* **200**, e00525-17 (2017). doi:10.1128/JB.00525-17 Medline

15. H. Nicoloff, V. Perreten, S. B. Levy, Increased genome instability in *Escherichia coli lon* mutants: Relation to emergence of multiple-antibiotic-resistant (Mar) mutants caused by insertion sequence elements and large tandem genomic amplifications. *Antimicrob. Agents Chemother.* **51**, 1293–1303 (2007). doi:10.1128/AAC.01128-06 Medline

16. H. Orlén, D. Hughes, Weak mutators can drive the evolution of fluoroquinolone resistance in *Escherichia coli*. *Antimicrob. Agents Chemother.* **50**, 3454–3456 (2006). doi:10.1128/AAC.00783-06 Medline

17. M. G. Reynolds, Compensatory evolution in rifampin-resistant *Escherichia coli*. *Genetics* **156**, 1471–1481 (2000). Medline

18. M. Oethinger, W. V. Kern, A. S. Jellen-Ritter, L. M. McMurry, S. B. Levy, Ineffectiveness of topoisomerase mutations in mediating clinically significant fluoroquinolone resistance in *Escherichia coli* in the absence of the AcrAB efflux pump. *Antimicrob. Agents Chemother.* **44**, 10–13 (2000). doi:10.1128/AAC.44.1.10-13.2000 Medline

19. J. A. Bohnert, S. Schuster, M. A. Seeger, E. Fähnrich, K. M. Pos, W. V. Kern, Site-directed mutagenesis reveals putative substrate binding residues in the *Escherichia coli* RND efflux pump AcrB. *J. Bacteriol.* **190**, 8225–8229 (2008). doi:10.1128/JB.00912-08 Medline

20. E. Denamur, I. Matic, Evolution of mutation rates in bacteria. *Mol. Microbiol.* **60**, 820–827 (2006). doi:10.1111/j.1365-2958.2006.05150.x Medline

21. S. Uphoff, N. D. Lord, B. Okumus, L. Potvin-Trottier, D. J. Sherratt, J. Paulsson, Stochastic activation of a DNA damage response causes cell-to-cell mutation rate variation. *Science* **351**, 1094–1097 (2016). doi:10.1126/science.aac9786 Medline

22. L. Robert, J. Ollion, J. Robert, X. Song, I. Matic, M. Elez, Mutation dynamics and fitness effects followed in single cells. *Science* **359**, 1283–1286 (2018). doi:10.1126/science.aan0797 Medline

23. S. Uphoff, Real-time dynamics of mutagenesis reveal the chronology of DNA repair and damage tolerance responses in single cells. *Proc. Natl. Acad. Sci. U.S.A.* **115**, E6516–E6525 (2018). doi:10.1073/pnas.1801101115

24. T. H. Wu, M. G. Marinus, Dominant negative mutator mutations in the *mutS* gene of *Escherichia coli*. *J. Bacteriol.* **176**, 5393–5400 (1994). doi:10.1128/jb.176.17.5393-5400.1994 Medline

25. K. B. Wood, P. Cluzel, Trade-offs between drug toxicity and benefit in the multi-antibiotic resistance system underlie optimal growth of *E. coli*. *BMC Syst. Biol.* **6**, 48 (2012). doi:10.1186/1752-0509-6-48 Medline

26. R. Krašovec, H. Richards, D. R. Gifford, C. Hatcher, K. J. Faulkner, R. V. Belavkin, A. Channon, E. Aston, A. J. McBain, C. G. Knight, Spontaneous mutation rate is a plastic trait associated with population density across domains of life. *PLOS Biol.* **15**, e2002731 (2017). doi:10.1371/journal.pbio.2002731 Medline

27. I. Nishimura, M. Kurokawa, L. Liu, B. W. Ying, Coordinated changes in mutation and growth rates induced by genome reduction. *mBio* **8**, e00676-17 (2017). doi:10.1128/mBio.00676-17 Medline

28. G. Feng, H. C. Tsui, M. E. Winkler, Depletion of the cellular amounts of the MutS and MutH methyl-directed mismatch repair proteins in stationary-phase *Escherichia coli* K-12 cells. *J. Bacteriol.* **178**, 2388–2396 (1996). doi:10.1128/jb.178.8.2388-2396.1996 Medline

29. T. M. Barbosa, S. B. Levy, Differential expression of over 60 chromosomal genes in *Escherichia coli* by constitutive expression of MarA. *J. Bacteriol.* **182**, 3467–3474 (2000). doi:10.1128/JB.182.12.3467-3474.2000 Medline

30. M. Baym, T. D. Lieberman, E. D. Kelsic, R. Chait, R. Gross, I. Yelin, R. Kishony, Spatiotemporal microbial evolution on antibiotic landscapes. *Science* **353**, 1147–1151 (2016). doi:10.1126/science.aag0822 Medline

31. K. Maneewannakul, S. B. Levy, Identification for *mar* mutants among quinolone-resistant clinical isolates of *Escherichia coli*. *Antimicrob. Agents Chemother.* **40**, 1695–1698 (1996). doi:10.1128/AAC.40.7.1695 Medline

32. N. A. Rossi, M. J. Dunlop, Customized regulation of diverse stress response genes by the multiple antibiotic resistance activator MarA. *PLOS Comput. Biol.* **13**, e1005310 (2017). doi:10.1371/journal.pcbi.1005310 Medline

33. S. Wang, Y. Wang, J. Shen, Y. Wu, C. Wu, Polymorphic mutation frequencies in clinical isolates of *Staphylococcus aureus*: The role of weak mutators in the development of fluoroquinolone resistance. *FEMS Microbiol. Lett.* **341**, 13–17 (2013). doi:10.1111/1574-6968.12085 Medline

34. P. Hsieh, K. Yamane, DNA mismatch repair: Molecular mechanism, cancer, and ageing. *Mech. Ageing Dev.* **129**, 391–407 (2008). doi:10.1016/j.mad.2008.02.012 Medline

35. M. M. Gottesman, I. H. Pastan, The role of multidrug resistance efflux pumps in cancer: Revisiting a *JNCI* publication exploring expression of the MDR1 (P-glycoprotein) gene. *J. Natl. Cancer Inst.* **107**, djv222 (2015). doi:10.1093/jnci/djv222 Medline

36. K. N. Adams, K. Takaki, L. E. Connolly, H. Wiedenhoft, K. Winglee, O. Humbert, P. H. Edelstein, C. L. Cosma, L. Ramakrishnan, Drug tolerance in replicating mycobacteria mediated by a macrophage-induced efflux mechanism. *Cell* **145**, 39–53 (2011). doi:10.1016/j.cell.2011.02.022 Medline

37. I. El Meouche, M. J. Dunlop, Data for: Heterogeneity in efflux pump expression predisposes antibiotic resistant cells to mutation, Dryad (2018); https://doi.org/10.5061/dryad.n1h9d0d.

38. F. R. Blattner, G. Plunkett 3rd, C. A. Bloch, N. T. Perna, V. Burland, M. Riley, J. Collado-Vides, J. D. Glasner, C. K. Rode, G. F. Mayhew, J. Gregor, N. W. Davis, H. A. Kirkpatrick, M. A. Goeden, D. J. Rose, B. Mau, Y. Shao, The complete genome sequence of *Escherichia coli* K-12. *Science* **277**, 1453–1462 (1997). doi:10.1126/science.277.5331.1453 Medline

39. K. A. Datsenko, B. L. Wanner, One-step inactivation of chromosomal genes in *Escherichia coli* K-12 using PCR products. *Proc. Natl. Acad. Sci. U.S.A.* **97**, 6640–6645 (2000). doi:10.1073/pnas.120163297 Medline

40. T. Baba, T. Ara, M. Hasegawa, Y. Takai, Y. Okumura, M. Baba, K. A. Datsenko, M. Tomita, B. L. Wanner, H. Mori, Construction of *Escherichia coli* K-12 in-frame, single-gene knockout mutants: The Keio collection. *Mol. Syst. Biol.* **2**, 0008 (2006). doi:10.1038/msb4100050 Medline

41. M. McClelland, K. E. Sanderson, J. Spieth, S. W. Clifton, P. Latreille, L. Courtney, S. Porwollik, J. Ali, M. Dante, F. Du, S. Hou, D. Layman, S. Leonard, C. Nguyen, K. Scott, A. Holmes, N. Grewal, E. Mulvaney, E. Ryan, H. Sun, L. Florea, W. Miller, T. Stoneking, M. Nhan, R. Waterston, R. K. Wilson, Complete genome sequence of *Salmonella enterica* serovar Typhimurium LT2. *Nature* **413**, 852–856 (2001). doi:10.1038/35101614 Medline

42. D. G. Gibson, L. Young, R.-Y. Chuang, J. C. Venter, C. A. Hutchison 3rd, H. O. Smith, Enzymatic assembly of DNA molecules up to several hundred kilobases. *Nat. Methods* **6**, 343–345 (2009). doi:10.1038/nmeth.1318 Medline

43. M. J. Dunlop, Z. Y. Dossani, H. L. Szmidt, H. C. Chu, T. S. Lee, J. D. Keasling, M. Z. Hadi, A. Mukhopadhyay, Engineering microbial biofuel tolerance and export using efflux pumps. *Mol. Syst. Biol.* **7**, 487 (2011). doi:10.1038/msb.2011.21 Medline

44. T. S. Lee, R. A. Krupa, F. Zhang, M. Hajimorad, W. J. Holtz, N. Prasad, S. K. Lee, J. D. Keasling, BglBrick vectors and datasheets: A synthetic biology platform for gene expression. *J. Biol. Eng.* **5**, 12 (2011). doi:10.1186/1754-1611-5-12 Medline

45. R. S. Cox 3rd, M. J. Dunlop, M. B. Elowitz, A synthetic three-color scaffold for monitoring genetic regulation and noise. *J. Biol. Eng.* **4**, 10 (2010). doi:10.1186/1754-1611-4-10 Medline

46. Y. Siu, J. Fenno, J. M. Lindle, M. J. Dunlop, Design and selection of a synthetic feedback loop for optimizing biofuel tolerance. *ACS Synth. Biol.* **7**, 16–23 (2018). doi:10.1021/acssynbio.7b00260 Medline

47. M. J. Dunlop, R. S. Cox 3rd, J. H. Levine, R. M. Murray, M. B. Elowitz, Regulatory activity revealed by dynamic correlations in gene expression noise. *Nat. Genet.* **40**, 1493–1498 (2008). doi:10.1038/ng.281 Medline

48. A. Gutierrez, L. Laureti, S. Crussard, H. Abida, A. Rodríguez-Rojas, J. Blázquez, Z. Baharoglu, D. Mazel, F. Darfeuille, J. Vogel, I. Matic, β-Lactam antibiotics

promote bacterial mutagenesis via an RpoS-mediated reduction in replication fidelity. *Nat. Commun.* **4**, 1610 (2013). doi:10.1038/ncomms2607 Medline

49. W. A. Rosche, P. L. Foster, Determining mutation rates in bacterial populations. *Methods* **20**, 4–17 (2000). doi:10.1006/meth.1999.0901 Medline

50. B. M. Hall, C. X. Ma, P. Liang, K. K. Singh, Fluctuation analysis CalculatOR: A web tool for the determination of mutation rate using Luria-Delbruck fluctuation analysis. *Bioinformatics* **25**, 1564–1565 (2009). doi:10.1093/bioinformatics/btp253 Medline

51. S. Stylianidou, C. Brennan, S. B. Nissen, N. J. Kuwada, P. A. Wiggins, SuperSegger: Robust image segmentation, analysis and lineage tracking of bacterial cells. *Mol. Microbiol.* **102**, 690–700 (2016). doi:10.1111/mmi.13486 Medline

52. L. Susman, M. Kohram, H. Vashistha, J. T. Nechleba, H. Salman, N. Brenner, Individuality and slow dynamics in bacterial growth homeostasis. *Proc. Natl. Acad. Sci. U.S.A.* **115**, E5679–E5687 (2018). doi:10.1073/pnas.1615526115 Medline